An Advanced Guide to Assembly and Operation of CO_2 Electrolyzers

Iglesias van Montfort, Hugo Pieter; Subramanian, Siddhartha; Irtem, Erdem; Sassenburg, Mark; Li, Mengran; Kok, Jesse; Middelkoop, Joost; Burdyny, Thomas

DOI
10.1021/acsenergylett.3c01561

Publication date
2023

Document Version
Final published version

Published in
ACS Energy Letters

Citation (APA)
Iglesias van Montfort, H. P., Subramanian, S., Irtem, E., Sassenburg, M., Li, M., Kok, J., Middelkoop, J., & Burdyny, T. (2023). An Advanced Guide to Assembly and Operation of CO_2 Electrolyzers. *ACS Energy Letters*, *8*(10), 4156-4161. https://doi.org/10.1021/acsenergylett.3c01561

ACS Energy LETTERS

http://pubs.acs.org/journal/aelccp

VIEWPOINT

An Advanced Guide to Assembly and Operation of CO_2 Electrolyzers

Cite This: *ACS Energy Lett.* 2023, 8, 4156–4161

Read Online

ACCESS | Metrics & More | Article Recommendations | Supporting Information

The electrochemical reduction of CO_2 is increasingly seen as a viable means of producing carbon-based fuels and feedstocks due to the rapid advancement of cost-linked performance metrics within the past decade. These rapid advancements have also uncovered many fundamental and applied challenges (e.g., salt formation, CO_2 utilization), which researchers have been systematically overcoming through various ingenuities at the catalyst, configuration, and operational levels.[1,2] Consequently, as the technology pushes further into the unknown and closer to commercially interesting performance metrics, the design, assembly, and operation of lab-scale CO_2 electrolyzers must be regimented. In fact, such regulation is now necessary just to achieve the relevant baseline data needed to demonstrate new performance advancements. While many research studies report their experimental cells and systems used to generate their novel results, few provide an extensive overview, protocol, and system diagram that allows new researchers to reconstruct the entirety of the electrolysis system. Groups or new researchers entering the CO_2 electrolysis research field must then either design systems themselves or incorporate pieces of information from a wide variety of sources.

In 2019 our research group provided an "introductory guide" to the assembly and operation of gas-diffusion electrodes for electrochemical CO_2 reduction that acted as a starting point for researchers to shift from aqueous-fed reactants in H-cells to gas-fed reactants using gas-diffusion layers.[3] At the time, we discussed the operational intricacies of rudimentary flow cells utilized at the time. The guide included cell assembly and operational details in the form of pictures and videos. In the past few years, however, substantial advancements have been made in the research field with regards to lab protocols, equipment, and product measurements that warrants an updated guide. Further, the previous guide did not discuss zero-gap membrane electrode assemblies (MEAs) in detail, which have now achieved widespread adoption in CO_2 electrolysis due to their cell simplicity and reduced ohmic losses. We then believe that the field would benefit from an updated "advanced guide" to the assembly and operation of gas-diffusion layers systems for the electrochemical reduction of CO_2.

In this Viewpoint, we present a comprehensive insight into our lab's materials, equipment, protocols, and methodology with the aim of providing a solid basis for further developments in the field. Additionally, we provide an in-depth start-up guide in our Supporting Information and video tutorials of assembly, start-up procedures and operation. The aim of this Viewpoint is to facilitate access to the CO_2-electrolysis field to accelerate advancements.

In the following section we provide an elaborate description of our cell designs and the use of gas-diffusion layers. We then detail the importance of accurate measurements and discuss our instrumentation setup used to control the electrolysis process. Finally, we provide additional information on analysis techniques and point the reader to detailed resources on various subtopics.

Background on the Use of Gas-Diffusion Layers. In the push for industrially feasible metrics, the CO_2 electrolysis field has steadily shifted from typical H-cell designs (where the reactant CO_2 is dissolved in the liquid catholyte) to catalysts supported on gas-diffusion electrodes (GDEs). These porous GDE substrates, usually carbon-based, drastically reduce the diffusion pathway for gaseous CO_2 to reach the catalyst, enabling high current densities and higher volumetric activity rates.

The use of GDEs with flowing catholytes (Figure 1a,b), however, is not without disadvantages. These systems are prone to flooding due to gas–liquid pressure imbalances, salt pumping and electrowetting,[4−6] leading some researchers to adopt gas-diffusion layers fully made of polytetrafluorethylene (PTFE).[7,8] In an architecture where reducing the diffusion length of CO_2 is key, flooding of GDEs hampers the performance and stability of these systems in the long term.

An answer to flooding concerns and high ohmic drops in catholytes can be found in MEA cells (Figure 1c,d) where the cathode and anode sandwich an ion-exchange membrane. The CO_2 reduction catalyst is then wetted while allowing for efficient CO_2 access from a GDE, and ionic species transport to and from the anode through a membrane. While MEAs reduce the risk of flooding, the low volume of water between the catalyst layer and the membrane increases the relative concentration of carbonate species considerably, which results in noticeable salt precipitation and accumulation, to the point that it can block the gas channels in the cathodic half-cell.

Received: July 31, 2023
Accepted: August 28, 2023
Published: September 14, 2023

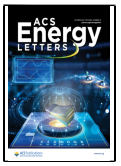

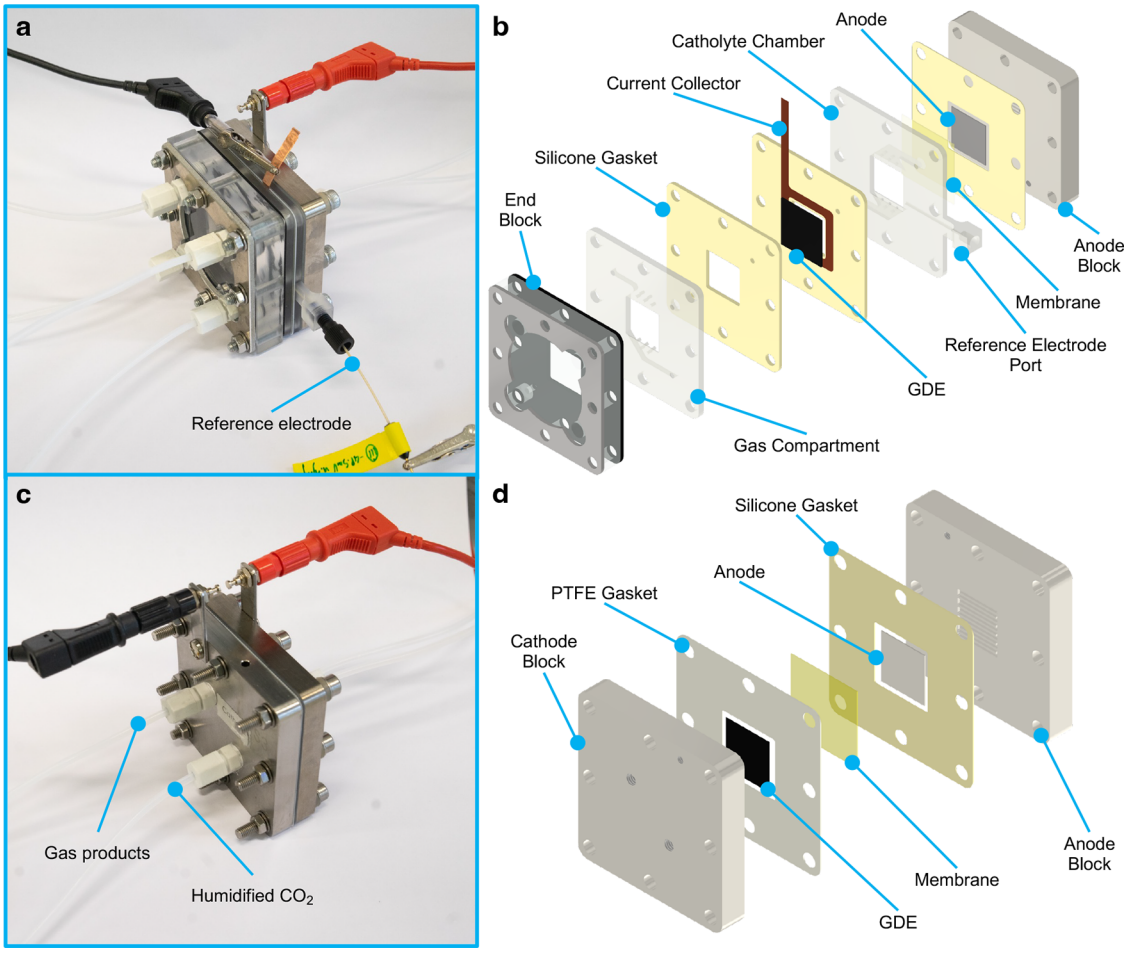

Figure 1. Lab-scale electrolyzers for CO_2RR characterization. (a) A flow electrolyzer, based on a commercial anode block and 3D-printed catholyte and gas channels, as assembled, and (b) in exploded view. (c) A commercially available MEA cell, as assembled, and (d) in exploded view.

Many of these challenges, however, are resolvable or manageable with proper system design and control strategies. Few resources provide such information. In this Viewpoint, we aim to illustrate the effects of stable operation of ancillary equipment of CO_2RR systems at a lab-scale, as well as displaying advances in diagnostic system integration in the test-bench.

Assembly and Operation of Flow Cells and MEA Cells for CO_2RR. In a flow-electrolyzer (FloE), a flowing catholyte along the cathode provides the medium for ions to be transported to the anode chamber. As the electrodes we intend to use for our application are of porous nature, a pressure equilibrium over the cathode is required to confine the electrode in the catholyte chamber and prevent any perspiration and flooding of the GDE, which would result in mass-transport limitations of the reactant CO_2 to the catalyst. The following section discusses the importance and challenges of this pressure regulation in detail.

The FloE design we present in this work is based around a 3D-printed catholyte flow field that accommodates a miniaturized leakless reference electrode (RE), as displayed in Figure 1a,b. 3D printing is an accessible solution to design and manufacture proprietary flow chambers, which allow for varying thicknesses and flow regimes along the GDE.[9] The inclusion of an RE allows one to operate the cathode at a specific set potential. In complex reaction systems where the applied overpotential determines the product distribution, being able to control the potential the potentiostat applies over the cathode is key to study the nature of the catalyst in detail. A step-by-step guide to assembly of this electrolyzer can be found in Supplementary Movie M1 and the Supporting Information.

As most potentiostats reported in the literature have a limited compliance voltage, minimizing cell voltage is key to ensuring high current densities can be evaluated at a lab scale. With this insight in mind, a reduction of the anodic and cathodic potentials required is essential. Our design achieves this by, first, employing an anode-design identical to that present in MEA cells (namely, a membrane adjacent to the employed anode and a serpentine flow-field through which the anolyte is circulated). Second, the thickness of the catholyte chamber is a mere 3 mm, which reduces the overpotential over the cathode chamber considerably when compared to designs prevalent in literature.[10,8] At the same time, the narrow catholyte channel allows the RE to be placed within 1 mm of the cathode, ensuring accurate control and sensing of the applied overpotential.

The MEA design presented in Figure 1c,d is similar to most reported in the literature and is based on commercially available solutions.[11] A titanium anode block with a milled serpentine channel and a similar stainless-steel cathode block clamp the membrane−electrode assembly, consisting of a Ni-

https://doi.org/10.1021/acsenergylett.3c01561
ACS Energy Lett. 2023, 8, 4156−4161

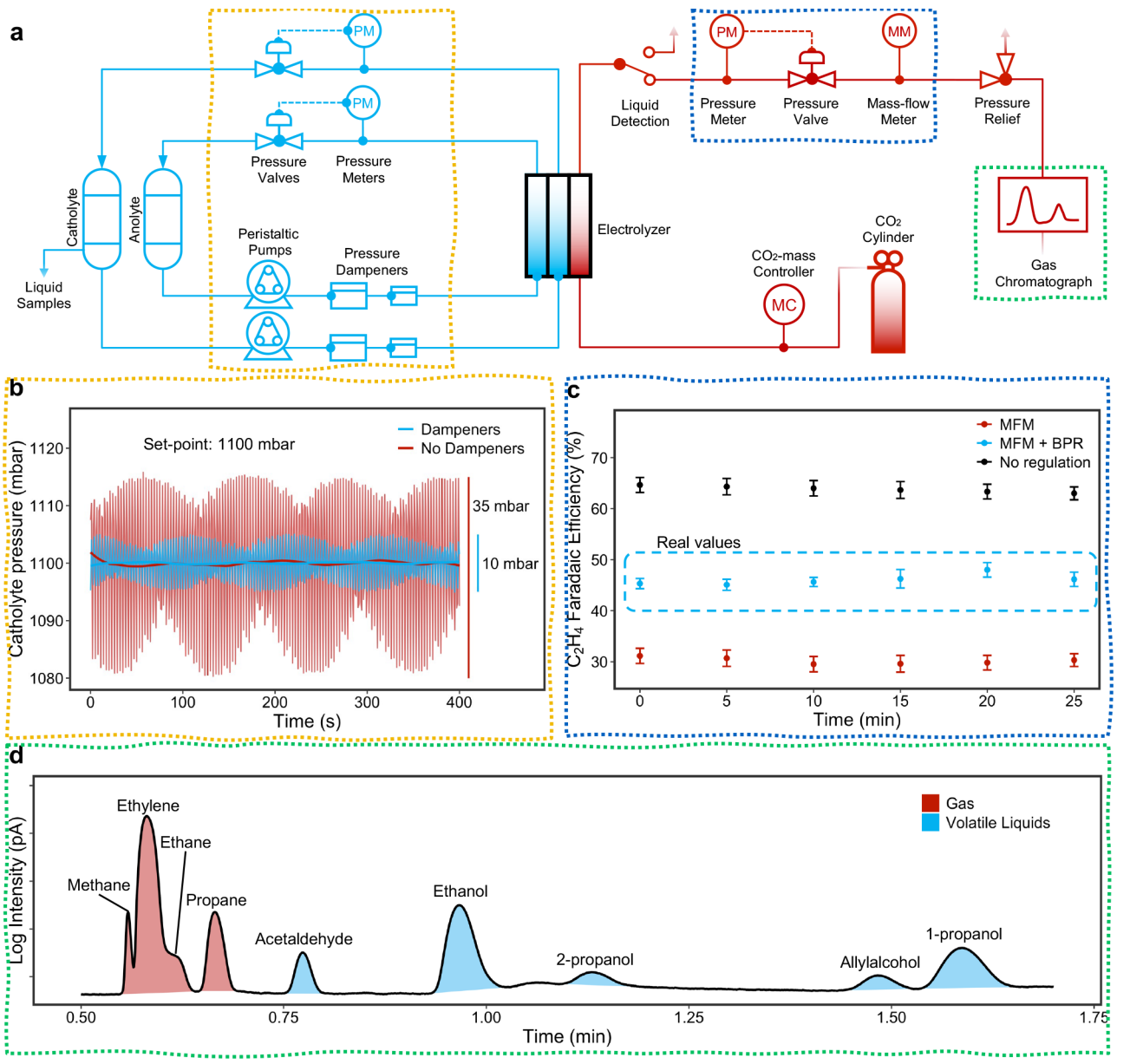

Figure 2. A reliable setup for studies on CO_2-electrolysis devices. (a) The process-flow diagram of a flow-cell setup, based on dampened liquid channels, a back-pressure regulator (BPR), and inline GC. (b) The inclusion of dampeners in the fluid channels helps reduce the impact of the peristaltic pumps' pressure spikes. (c) Not regulating and measuring the exit-flow rate results in overestimation of Faradaic efficiencies, as shown in black. On the other hand, just measuring the exit flow rate results in underestimation, as gas leaks to the catholyte compartment (in red). CO_2 electrolysis requires a BPR and mass-flow meter (MFM) that both regulate the pressure difference over the GDE and measure the product flow rate (in blue). (d) Gas chromatography is an adequate method for estimating Faradaic efficiencies of volatile liquid products, as are those of copper catalysts.

foam, an anion-exchange membrane, and a GDE-based cathode. A visual and assembly guide of this architecture is included in Supplementary Movie M2. The Supporting Information includes a step-by-step description of the start-up protocol.

Regulation and Measurement of Flow and Pressure in Liquid and Gas Compartments of the Electrolyzer. As discussed above, GDE-based FloE and MEA systems require a stable interface at the cathode to operate in a sustainable manner.[12,13] Control over the inlet flows and pressures of the various gas and liquid channels of the electrolyzer is then essential. Additionally, due to large differences in the inlet to outlet gas flow rates caused by imbalanced CO_2 consumption and product evolution, the flow rate of the CO_2 outlet stream must be measured near or at the point of product quantification to accurately determine gaseous Faradaic efficiencies.[14,15] Both the stability and product measurement aspects then require substantial balance of plant equipment and calibration to be able to accurately reports traditional CO_2RR metrics. In this section and in the Supporting Information we discuss these in detail.

Within our test setup we control all gas and liquid pressures in the electrolyzer using a combination of pumps, dampeners, and back-pressure regulators (see Figure 2a). The electrolyte, contained in a reservoir, is pumped continuously using a peristaltic pump. Since these pumps cause oscillatory pressure

https://doi.org/10.1021/acsenergylett.3c01561
ACS Energy Lett. 2023, 8, 4156−4161

spikes in the stream, we included two dampeners per fluid stream to reduce pulsation amplitudes. The electrolyte then flows through the electrolyzer and exits toward a back-pressure regulator (BPR). The BPR consists of a pressure meter coupled to a controller (a valve) that regulates the pressure of the stream in real-time through a proprietary software application. The combined pump, pressure dampener, and BPR limit liquid pressure oscillations of the electrolyte channels considerably, especially at elevated pressures, as can be seen in Figure 2b. A thorough overview and operation guide can be found in the Supporting Information, as well as Supplementary Movie M3.

A similar pressure-regulation device is also required in the gas channel of our setup (Figure 2a). When combined the gas and liquid BPRs allow for the absolute and differential pressures of each channel to be regulated, preventing unnecessary gas−liquid crossover across the GDE during operation. Without differential pressure control of the gas−liquid channel, periodic gas penetration into the liquid channel is particularly problematic as it results in periodic perturbations in the gas flow rate, hindering accurate product quantification. Gas crossover across the GDE into the liquid phase will occur at extremely small gas overpressures, thus requiring a liquid overpressure between 10 and 30 mbar to be set for flowing catholyte systems. Such pressure control is less important for MEA systems due to the polymer membrane blocking direct gas crossover.

A final critical measurement component is a mass flow meter (MFM) or nitrogen bleed into the gas chromatograph (GC) to measure the real flow rate leaving the electrochemical cell. In both neutral-pH and alkaline CO_2 electrolyzers substantial gaseous CO_2 is consumed by abundant hydroxide byproducts of electrolysis, causing outlet flow rates to be lower than inputted values. Further, hydrogen evolution can increase flow rates while multicarbon products consume 2 (or more) mols of CO_2 per 1 mol of gas evolved. These factors then require the outlet gas stream to be accurately measured and recorded. When using a mass flow meter, which is typically calibrated for a specific gas, the measured outlet flow then also must be corrected by the gas composition determined by the GC (see Supporting Information).[16]

In Figure 2c we briefly highlight the need for both a gas-phase BPR and measurement of the gas flow rate (either via a mass flow meter or a nitrogen bleed to the gas chromatograph). Here we can see three sets of measured data for CO_2RR on sputtered Cu electrodes in 1 M $KHCO_3$. In the black data points the ethylene Faradaic efficiency appears overrepresented due to the use of the inlet flow rate of CO_2 instead of the outlet gas flow rate in the calculation. Further, the red data show that when a MFM is used without a BPR, gas crossover into the liquid phase results in an under-representation of the formed products. Lastly, a combined implementation of an MFM and a BPR system shows the true measured ethylene Faradaic efficiency close to the true values (Figure 2c, in blue). We provide, in the Supporting Information and Movie M3, start-up protocols that are followed to ensure gas−liquid balances, proper pressure regulation, and cell start-up. This combined approach to measuring and regulating the effluent streams removes one of the major pitfalls in catalyst evaluation in the CO_2 electrolysis field.[17]

Integration of In-Line Diagnostic Systems. Key performance metrics of CO_2RR systems in the literature include, among many, energy and Faradaic efficiency toward products, single-pass conversion rate of CO_2, and long-term stability and selectivity of the cathode.[18] A big part of these metrics revolves around identification and quantification of the species present in the effluent product stream of the electrolyzer. Ensuring that the measurement of all products is as accurate and speedy as possible is then crucial for reporting the performance of CO_2RR electrolyzers.[19] Since products of the electrolyzer can either be gaseous (e.g., carbon monoxide, methane, ethylene) or liquid (e.g., formate, ethanol, acetate), each stream requires separate analysis methods.

Gaseous products are commonly analyzed using a gas chromatograph (GC).[20] This technique separates a gas stream and analyzes its composition as a function of its residence time in separation columns (see the Supporting Information for a detailed description). Whereas some reports in the literature involve a manual injection of effluent gas into the GC,[21,22] our setup has an automatic injection method that periodically collects samples from the gas stream leaving the electrolyzer. This allows us to screen the species in the outlet gas every 5 min without margin for human or mechanical error during injection. Recent reports have shown the advantage of using infrared-based detection methods, which increase the scanning frequency and avoid typical shortcomings of GCs, like sensitivity to liquid and salt accumulation.[23,24]

For the analysis of liquid products, we use high-performance liquid chromatography (HPLC), which uses a system similar to a GC to separate liquid species in an acidic carrying solvent (see the Supporting Information). This allows us to separate most CO_2RR products, even for complex catalysts as copper.[25] The relative tolerance to basic solutions (pH $\leq$ 13, approximately) makes this a more intuitive and accessible method than nuclear-magnetic resonance (NMR), more prevalent in the field,[26−28] which requires extensive sample preparation and cleaning of analysis tubes. Most of these liquid products have a high-enough volatility to be detected in the gaseous stream (see Figure 2d). While saturation times for these products are noticeably higher than those of their gaseous counterparts, signaling using the GC is an adequate proxy for quick assessment of the performance of a cathode (see the Supporting Information).

Identification of the reactant for a specific product made with low concentrations is best carried out by using labeled CO_2 (C^{13}-based dioxide) to ensure the product is not a result of contamination and is in fact coming from gaseous CO_2.[29] Gas-chromatography systems, however, do not possess sufficient resolution to separate labeled isotopes in products. Instead, combined use of gas-chromatography and mass-spectrometry (MS) systems is common practice in the field.[30] Alternatively, online electrochemical mass spectrometry (OLEMS) provides a flexible architecture that is capable of identifying gas-fraction products of CO_2RR at a high refresh-rate.[31−34]

Additional Detailed Resources for Various Measurement Aspects. Beyond the information provided here, several other articles have performed various deep dives in advanced measurements and characterization, which we would like to point the reader to. For example, near-unity product analysis and full carbon balances can be extremely challenging in MEA and flowing electrolyzers. While we have highlighted some best practices here, even more advanced methods exist to, for example, (i) separately quantify ^{12}C versus ^{13}C products and hard to detect formaldehyde,[35] (ii) fully quantify liquid

https://doi.org/10.1021/acsenergylett.3c01561
ACS Energy Lett. 2023, 8, 4156−4161

products that can vaporize into the gas stream or crossover to the anode,[36] (iii) accurately measure the potential-drops over every component in a zero-gap MEA electrolyzer,[37] (iv) segment a flow field to observe geometric product distributions,[38] and (v) analyze the kinetics of CO_2 electrolysis in an advanced reactor design using electrochemical impedance spectroscopy (EIS).[39]

In summary, this Viewpoint presents a comprehensive look into our lab-scale operation and analysis protocols of CO_2 electrolyzers. Setups and observations made in the study of these electrolyzers are not trivial and not one-to-one translatable from prior knowledge in other electrochemical fields like water electrolysis and hydrogen fuel cells. By highlighting our advances in cell design, process-flow implementation and control, and product quantification, we aim to provide a solid starting base for anyone looking to contribute to the scientific advancement of this field. This document should then become a stepping stone for anyone without prior experience in the electrochemical conversion of CO_2.

Hugo-Pieter Iglesias van Montfort orcid.org/0000-0002-9594-392X
Siddhartha Subramanian orcid.org/0000-0002-7992-3849
Erdem Irtem orcid.org/0000-0002-2730-8932
Mark Sassenburg orcid.org/0000-0002-2826-7765
Mengran Li orcid.org/0000-0001-7858-0533
Jesse Kok
Joost Middelkoop
Thomas Burdyny orcid.org/0000-0001-8057-9558

■ ASSOCIATED CONTENT

Supporting Information

The Supporting Information is available free of charge at https://pubs.acs.org/doi/10.1021/acsenergylett.3c01561.

Equipment guide for CO_2 electrolysis on a lab-scale, materials and methods, troubleshooting guide, supporting references (PDF)

Assembly of a lab-scale flow electrolyzer for CO_2 electrolysis (MP4)

Assembly of a zero-gap membrane-electrode assembly for CO_2 electrolysis (MP4)

Testing bench walkthrough and startup procedure of a flow electrolyzer (MP4)

■ AUTHOR INFORMATION

Complete contact information is available at: https://pubs.acs.org/10.1021/acsenergylett.3c01561

Notes

Views expressed in this Viewpoint are those of the authors and not necessarily the views of ACS.
The authors declare no competing financial interest.

■ ACKNOWLEDGMENTS

H-P.I.v.M. and T.B. acknowledge the financing provided for this project in the context of the e-Refinery Institute by Shell Global Solutions International B.V. and the Top Consortia for Knowledge and Innovation (TKIs) of the Dutch Ministry of Economic Affairs. M.L. acknowledges the financial support of the Australian Research Council (DE230100637).

■ REFERENCES

(1) Salvatore, D. A.; Weekes, D. M.; He, J.; Dettelbach, K. E.; Li, Y. C.; Mallouk, T. E.; Berlinguette, C. P. Electrolysis of Gaseous CO_2 to CO in a Flow Cell with a Bipolar Membrane. *ACS Energy Lett.* **2018**, *3* (1), 149−154.
(2) Yang, K.; Li, M.; Subramanian, S.; Blommaert, M. A.; Smith, W. A.; Burdyny, T. Cation-Driven Increases of CO_2 Utilization in a Bipolar Membrane Electrode Assembly for CO_2 Electrolysis. *ACS Energy Lett.* **2021**, *6* (12), 4291−4298.
(3) Liu, K.; Smith, W. A.; Burdyny, T. Introductory Guide to Assembling and Operating Gas Diffusion Electrodes for Electrochemical CO_2 Reduction. *ACS Energy Lett.* **2019**, *4*, 639.
(4) Kim, J.-H.; Lee, J.-H.; Mirzaei, A.; Kim, H. W.; Tan, B. T.; Wu, P.; Kim, S. S. Electrowetting-on-Dielectric Characteristics of ZnO Nanorods. *Sci. Rep.* **2020**, *10* (1), 14194.
(5) Baumgartner, L. M.; Koopman, C. I.; Forner-Cuenca, A.; Vermaas, D. A. Narrow Pressure Stability Window of Gas Diffusion Electrodes Limits the Scale-Up of CO2 Electrolyzers. *ACS Sustain. Chem. Eng.* **2022**, *10* (14), 4683−4693.
(6) Baumgartner, L. M.; Koopman, C. I.; Forner-Cuenca, A.; Vermaas, D. A. When Flooding Is Not Catastrophic—Woven Gas Diffusion Electrodes Enable Stable CO_2 Electrolysis. *ACS Appl. Energy Mater.* **2022**, *5* (12), 15125−15135.
(7) Dinh, C.-T.; Burdyny, T.; Kibria, M. G.; Seifitokaldani, A.; Gabardo, C. M.; Garcia de Arquer, F. P.; Kiani, A.; Edwards, J. P.; De Luna, P.; Bushuyev, O. S.; Zou, C.; Quintero-Bermudez, R.; Pang, Y.; Sinton, D.; Sargent, E. H. CO_2 Electroreduction to Ethylene via Hydroxide-Mediated Copper Catalysis at an Abrupt Interface. *Science* **2018**, *360*, 783−787.
(8) García de Arquer, F. P.; Dinh, C. T.; Ozden, A.; Wicks, J.; McCallum, C.; Kirmani, A. R.; Nam, D. H.; Gabardo, C.; Seifitokaldani, A.; Wang, X.; Li, Y. C.; Li, F.; Edwards, J.; Richter, L. J.; Thorpe, S. J.; Sinton, D.; Sargent, E. H. CO_2 Electrolysis to Multicarbon Products at Activities Greater than 1 A cm^{-2}. *Science* **2020**, *367*, 661−666.
(9) Corral, D.; Feaster, J. T.; Sobhani, S.; DeOtte, J. R.; Lee, D. U.; Wong, A. A.; Hamilton, J.; Beck, V. A.; Sarkar, A.; Hahn, C.; Jaramillo, T. F.; Baker, S. E.; Duoss, E. B. Advanced Manufacturing for Electrosynthesis of Fuels and Chemicals from CO_2. *Energy Environ. Sci.* **2021**, *14* (5), 3064−3074.
(10) Löwe, A.; Rieg, C.; Hierlemann, T.; Salas, N.; Kopljar, D.; Wagner, N.; Klemm, E. Influence of Temperature on the Performance of Gas Diffusion Electrodes in the CO_2 Reduction Reaction. *ChemElectroChem.* **2019**, *6* (17), 4497−4506.
(11) Kaczur, J. J.; Yang, H.; Liu, Z.; Sajjad, S. D.; Masel, R. I. Carbon Dioxide and Water Electrolysis Using New Alkaline Stable Anion Membranes. *Front. Chem.* **2018**, *6*, 263.
(12) Deng, W.; Zhang, L.; Li, L.; Chen, S.; Hu, C.; Zhao, Z.-J.; Wang, T.; Gong, J. Crucial Role of Surface Hydroxyls on the Activity and Stability in Electrochemical CO $_2$ Reduction. *J. Am. Chem. Soc.* **2019**, *141* (7), 2911−2915.
(13) Xu, Y.; Edwards, J. P.; Liu, S.; Miao, R. K.; Huang, J. E.; Gabardo, C. M.; O'Brien, C. P.; Li, J.; Sargent, E. H.; Sinton, D. Self-Cleaning CO_2 Reduction Systems: Unsteady Electrochemical Forcing Enables Stability. *ACS Energy Lett.* **2021**, *6* (2), 809−815.
(14) Ma, M.; Clark, E. L.; Therkildsen, K. T.; Dalsgaard, S.; Chorkendorff, I.; Seger, B. Insights into the Carbon Balance for CO_2 Electroreduction on Cu Using Gas Diffusion Electrode Reactor Designs. *Energy Environ. Sci.* **2020**, *13* (3), 977−985.
(15) Niu, Z.-Z.; Chi, L.-P.; Liu, R.; Chen, Z.; Gao, M.-R. Rigorous Assessment of CO_2 Electroreduction Products in a Flow Cell. *Energy Environ. Sci.* **2021**, *14* (8), 4169−4176.
(16) Subramanian, S.; Middelkoop, J.; Burdyny, T. Spatial Reactant Distribution in CO_2 Electrolysis: Balancing CO_2 Utilization and Faradaic Efficiency. *Sustain. Energy Fuels* **2021**, *5* (23), 6040−6048.
(17) Tan, Y. C.; Quek, W. K.; Kim, B.; Sugiarto, S.; Oh, J.; Kai, D. Pitfalls and Protocols: Evaluating Catalysts for CO_2 Reduction in Electrolyzers Based on Gas Diffusion Electrodes. *ACS Energy Lett.* **2022**, *7* (6), 2012−2023.

(18) Wakerley, D.; Lamaison, S.; Wicks, J.; Clemens, A.; Feaster, J.; Corral, D.; Jaffer, S. A.; Sarkar, A.; Fontecave, M.; Duoss, E. B.; Baker, S.; Sargent, E. H.; Jaramillo, T. F.; Hahn, C. Gas Diffusion Electrodes, Reactor Designs and Key Metrics of Low-Temperature CO_2 Electrolysers. *Nat. Energy* **2022**, *7* (2), 130−143.
(19) Seger, B.; Robert, M.; Jiao, F. Best Practices for Electrochemical Reduction of Carbon Dioxide. *Nat. Sustain.* **2023**, *6* (3), 236−238.
(20) Diercks, J. S.; Pribyl-Kranewitter, B.; Herranz, J.; Chauhan, P.; Faisnel, A.; Schmidt, T. J. An Online Gas Chromatography Cell Setup for Accurate CO_2 -Electroreduction Product Quantification. *J. Electrochem. Soc.* **2021**, *168* (6), 064504.
(21) García De Arquer, F. P.; Bushuyev, O. S.; De Luna, P.; Dinh, C.-T.; Seifitokaldani, A.; Saidaminov, M. I.; Tan, C.-S.; Quan, L. N.; Proppe, A.; Kibria, Md. G.; Kelley, S. O.; Sinton, D.; Sargent, E. H. 2D Metal Oxyhalide-Derived Catalysts for Efficient CO_2 Electroreduction. *Adv. Mater.* **2018**, *30* (38), 1802858.
(22) Huang, J. E.; Li, F.; Ozden, A.; Sedighian Rasouli, A.; García de Arquer, F. P.; Liu, S.; Zhang, S.; Luo, M.; Wang, X.; Lum, Y.; Xu, Y.; Bertens, K.; Miao, R. K.; Dinh, C.-T.; Sinton, D.; Sargent, E. H. CO_2 Electrolysis to Multicarbon Products in Strong Acid. *Science* **2021**, *372* (6546), 1074−1078.
(23) Samu, A. A.; Szenti, I.; Kukovecz, A.; Endrodi, B.; Janaky, C. Systematic Screening of Gas Diffusion Layers for High Performance CO_2 Electrolysis. *Commun. Chem.* **2023**, *6* (1), 41.
(24) Samu, A. A.; Kormányos, A.; Kecsenovity, E.; Szilágyi, N.; Endrődi, B.; Janáky, C. Intermittent Operation of CO_2 Electrolyzers at Industrially Relevant Current Densities. *ACS Energy Lett.* **2022**, *7* (5), 1859−1861.
(25) Sassenburg, M.; de Rooij, R.; Nesbitt, N. T.; Kas, R.; Chandrashekar, S.; Firet, N. J.; Yang, K.; Liu, K.; Blommaert, M. A.; Kolen, M.; Ripepi, D.; Smith, W. A.; Burdyny, T. Characterizing CO_2 Reduction Catalysts on Gas Diffusion Electrodes: Comparing Activity, Selectivity, and Stability of Transition Metal Catalysts. *ACS Appl. Energy Mater.* **2022**, *5* (5), 5983−5994.
(26) Morales-Guio, C. G.; Cave, E. R.; Nitopi, S. A.; Feaster, J. T.; Wang, L.; Kuhl, K. P.; Jackson, A.; Johnson, N. C.; Abram, D. N.; Hatsukade, T.; Hahn, C.; Jaramillo, T. F. Improved CO_2 Reduction Activity towards C2+ Alcohols on a Tandem Gold on Copper Electrocatalyst. *Nat. Catal.* **2018**, *1* (10), 764−771.
(27) Hoang, T. T. H.; Verma, S.; Ma, S.; Fister, T. T.; Timoshenko, J.; Frenkel, A. I.; Kenis, P. J. A.; Gewirth, A. A. Nanoporous Copper-Silver Alloys by Additive-Controlled Electrodeposition for the Selective Electroreduction of CO_2 to Ethylene and Ethanol. *J. Am. Chem. Soc.* **2018**, *140* (17), 5791−5797.
(28) Zhang, T.; Bui, J. C.; Li, Z.; Bell, A. T.; Weber, A. Z.; Wu, J. Highly Selective and Productive Reduction of Carbon Dioxide to Multicarbon Products via in Situ CO Management Using Segmented Tandem Electrodes. *Nat. Catal.* **2022**, *5* (3), 202−211.
(29) Wang, X.; de Araújo, J. F.; Ju, W.; Bagger, A.; Schmies, H.; Kühl, S.; Rossmeisl, J.; Strasser, P. Mechanistic Reaction Pathways of Enhanced Ethylene Yields during Electroreduction of CO_2-CO Co-Feeds on Cu and Cu-Tandem Electrocatalysts. *Nat. Nanotechnol.* **2019**, *14* (11), 1063−1070.
(30) Liu, C.; Nangle, S. N.; Colón, B. C.; Silver, P. A.; Nocera, D. G. ^{13} C-Labeling the Carbon-Fixation Pathway of a Highly Efficient Artificial Photosynthetic System. *Faraday Discuss.* **2017**, *198*, 529−537.
(31) Kas, R.; Kortlever, R.; Milbrat, A.; Koper, M. T. M.; Mul, G.; Baltrusaitis, J. Electrochemical CO_2 Reduction on Cu_2 O-Derived Copper Nanoparticles: Controlling the Catalytic Selectivity of Hydrocarbons. *Phys. Chem. Chem. Phys.* **2014**, *16* (24), 12194−12201.
(32) Shen, J.; Kortlever, R.; Kas, R.; Birdja, Y. Y.; Diaz-Morales, O.; Kwon, Y.; Ledezma-Yanez, I.; Schouten, K. J. P.; Mul, G.; Koper, M. T. M. Electrocatalytic Reduction of Carbon Dioxide to Carbon Monoxide and Methane at an Immobilized Cobalt Protoporphyrin. *Nat. Commun.* **2015**, *6* (1), 8177.
(33) Todoroki, N.; Tsurumaki, H.; Tei, H.; Mochizuki, T.; Wadayama, T. Online Electrochemical Mass Spectrometry Combined with the Rotating Disk Electrode Method for Direct Observations of Potential-Dependent Molecular Behaviors in the Electrode Surface Vicinity. *J. Electrochem. Soc.* **2020**, *167* (10), 106503.
(34) Zhang, G.; Cui, Y.; Kucernak, A. Real-Time In Situ Monitoring of CO_2 Electroreduction in the Liquid and Gas Phases by Coupled Mass Spectrometry and Localized Electrochemistry. *ACS Catal.* **2022**, *12* (10), 6180−6190.
(35) Chatterjee, T.; Boutin, E.; Robert, M. Manifesto for the Routine Use of NMR for the Liquid Product Analysis of Aqueous CO_2 Reduction: From Comprehensive Chemical Shift Data to Formaldehyde Quantification in Water. *Dalton Trans.* **2020**, *49* (14), 4257−4265.
(36) Zhang, J.; Luo, W.; Züttel, A. Crossover of Liquid Products from Electrochemical CO_2 Reduction through Gas Diffusion Electrode and Anion Exchange Membrane. *J. Catal.* **2020**, *385*, 140−145.
(37) Hansen, K. U.; Cherniack, L. H.; Jiao, F. Voltage Loss Diagnosis in CO_2 Electrolyzers Using Five-Electrode Technique. *ACS Energy Lett.* **2022**, *7* (12), 4504−4511.
(38) Simonson, H.; Klein, W. E.; Henckel, D.; Verma, S.; Neyerlin, K. C.; Smith, W. A. Direct Measurement of Electrochemical Selectivity Gradients over a 25 cm^2 Copper Gas Diffusion Electrode. *ACS Energy Lett.* **2023**, 3811−3819.
(39) Bienen, F.; Kopljar, D.; Löwe, A.; Geiger, S.; Wagner, N.; Klemm, E.; Friedrich, K. A. Revealing Mechanistic Processes in Gas-Diffusion Electrodes During CO_2 Reduction via Impedance Spectroscopy. *ACS Sustain. Chem. Eng.* **2020**, *8* (36), 13759−13768.

https://doi.org/10.1021/acsenergylett.3c01561
ACS Energy Lett. 2023, 8, 4156−4161